Contemporary Mathematics
https://ojs.wiserpub.com/index.php/CM/

Research Article

An q-Rung Orthopair Trapezoidal Fuzzy Number Decision-Making Method for Online Learning Engagement Assessment

Benting Wan[1*], Jiachen Sun[1], Haifeng Du[2], Jun Wan[1], Xiangwen Kong[1], Youyu Cheng[1]

[1] School of Software and IoT Engineering, Jiangxi University of Finance and Economics, Nanchang, 330013, China
[2] Beijing Qianfeng Internet Technology Company, Beijing, 10083, China
E-mail: wanbenting@jxufe.edu.cn

Received: 5 August 2025; **Revised:** 9 October 2025; **Accepted:** 10 November 2025

Abstract: Student engagement in online learning is very important for assessing learning effectiveness. However, the process of learners' engagement, including its rise, stability, and decline, is complex and uncertain. Therefore, the student's online learning engagement assessment method is developed based on q-Rung Orthogonal Trapezoidal Fuzzy Numbers (q-ROFTrNs) in this paper. First, an q-rung orthogonal trapezoidal fuzzy Yager operator is designed. Second, a derived feature weight method is developed based on the Criteria Importance Through Intercriteria Correlation (CRITIC) under the q-ROFTrNs environment, which not only overcomes the shortcomings of specified weights but also has objectivity. Third, an integrated q-Rung Orthogonal Trapezoidal Fuzzy Number Decision-Making (q-ROFTrNDM) method is explored. This method combines fuzzy distance, Yager operator, CRITIC method, and score function to achieve a comprehensive and dynamic assessment of students' engagement. The assessment results of the q-ROFTrNDM method indicate that students' online learning engagement aligns with expert assessment outcomes. Parameter sensitivity analysis reveals that the proposed q-ROFTrNDM method does not alter the assessment results of the most engaged students. Comparative analysis demonstrates that q-ROFTrNDM achieves a higher engagement score than 0.929, outperforming competing methods. Additionally, the q-ROFTrNDM method boasts a computation time of less than 10 ms. Therefore, the implementation outcomes confirm the feasibility and effectiveness of q-ROFTrNDM.

***Keywords*:** Yager operator, online learning, q-rung orthopair trapezoidal fuzzy number, Criteria Importance Through Intercriteria Correlation (CRITIC)

MSC: 47A08, 97U11

1. Introduction

Decision-Making (DM) methods have been widely applied in complex, ambiguous, and dynamic environments. Many classical DM methods exist, such as Technique for Order Preference by Similarity to Ideal Solution (TOPSIS), Criteria Importance Through Intercriteria Correlation (CRITIC) [1]. These methods have been applied in decision assessment, and with the development of fuzzy sets, corresponding DM methods have also emerged [2]. Since Zadeh proposed the concept of fuzzy sets, fuzzy theory has been widely applied to Multi-Attribute Decision-Making (MADM) [3]. To represent the attitude information of decision-makers, Atanassov further proposed Intuitionistic Fuzzy Sets (IFS)

DOI: https://doi.org/10.37256/cm.7220268156

[4], which is an attractive approach to dealing with fuzzy and inaccurate data. IFS is defined by membership (u) and non-membership (v), and $u+v \leq 1$ [5]. Yager further introduced the Pythagoras Fuzzy Sets (PFS) [6, 7] and q-Rung Orthopair Fuzzy Sets (q-ROFS) [8] as useful extensions of IFS and PFS, where $((u)^q+(v)^q \leq 1)$ [9]. As the value of q increases, the q-ROFS becomes more suitable for uncertain environments [10]. With the development of fuzzy sets, researchers have developed Trapezoidal Fuzzy Number (TrFN) and triangular fuzzy numbers. The TrFN can well represent the dynamic processes of rising, stable, and falling. Therefore, it has received significant engagement from researchers, and different TrFN with different fuzzy sets have been developed, such as TrFNs [11], Trapezoidal Intuitionistic Fuzzy Sets (TrIFNs) [12], etc. However, in some cases, TrFN does not fully meet the requirements of real DM, where the $u+v>1$ [13]. To address this issue, inspired by the ideas of q-ROFS and TrFNs, researchers introduced the q-rung Orthopair Trapezoidal Fuzzy Numbers (q-ROFTrNs) [14]. The membership degree of the developed q-ROFTrNs is the same as that of TrFNs, and it can well represent the dynamic processes of rising, stable, and falling. Moreover, the non-membership degree of q-ROFTrNs can capture dynamic patterns of decline, stability, and rise [15]. Compared with TrIFNs, q-ROFTrNs need to satisfy $(u)^q+(v)^q \leq 1$. Therefore, it provides more freedom for decision-makers. At the same time, the membership degree change process of q-ROFTrNs is similar to the state change process of learners during online learning. However, the research on using q-ROFTrNs to represent engagement degree requires further exploration. This paper will examine the q-ROFTrNs representation features of online learning engagement degree [16].

In the process of MADM, it is necessary to aggregate the opinions of different experts; the aggregation operator is used to fuse the opinions of different experts [17]. For this purpose, researchers have developed a large number of aggregation operators, such as weighted average, Yager, Bonferroni Mean (BM), etc [18–20]. Among them, the Yager operator [20] is an operator commonly used in fuzzy reasoning and DM. It has the advantages and characteristics of nonlinearity, robustness, adjustability, representativeness, and ease of understanding, and is suitable for fuzzy reasoning and DM problems in various fuzzy environments [21]. In different fuzzy sets, the Yager operator has also been extended, such as the Zadeh fuzzy Yager operator, intuitionistic fuzzy Yager operator, q-rung orthogonal Yager operator, and interval-valued q-rung orthogonal Yager operator. However, there is currently no research on Yager operators under the q-ROFTrNs environment. This paper will address this gap and apply it to aggregate information in MADM.

However, in the process of aggregating information, the attribute weights are the key for DM. Therefore, researchers have proposed a large number of methods for deriving attribute weight. There are subjective methods, such as the Analytic Hierarchy Process (AHP) [22] and judgment matrices [23]. And objective methods, such as entropy weight, deviation maximization, variance maximization, CRITIC, etc [24, 25]. Among them, the CRITIC is objective and efficient, and is often used to derive real-time weight in objective environments [26, 27]. Since the engagement assessment of online learning often requires feedback, this paper will adopt the CRITIC method to derive the feature weights of student online learning engagement.

As a key indicator of cognitive engagement in online learning, engagement not only reflects learning efficiency but also provides feedback for teaching strategies. However, current research faces two major challenges. The lack of a unified definition of the multi-dimensional characteristics of engagement hinders the standardization of assessment, and the large class size and limited monitoring capabilities highlight the limitations of traditional methods (manual observation), which are highly subjective and imprecise. Assessing the online learning engagement often requires consideration of multiple features [28]. Existing research commonly uses individual features such as facial cues, gaze, posture, and head position, or combines multiple features [29]. In the context of multiple features, researchers proposed engagement assessment methods that integrate multimodal, heterogeneous data-especially through the fusion of facial and physiological data. These methods commonly rely on deep learning networks that have long learning times and low efficiency, and room for improvement in accuracy [30]. As a result, some scholars have proposed a fuzzy fusion method [31], which offers greater efficiency. However, most existing fuzzy assessment models are based on Zadeh fuzzy sets, which limits the precision of the assessment. Therefore, the q-ROFTrNs is used to represent features and develop an operator to fuse data of various features.

To sum up, the Yager operators and the CRITIC method demonstrate strong applicability in practical DM problems. However, Yager operators and the CRITIC method remain underdeveloped within the q-ROFTrN environment. However, there are still some research gaps that remain unresolved. Therefore, the main motivations for this study are as follows.

(1) Although q-ROFTrNs have been widely promoted and applied, the Yager operator has yet to be developed under the q-ROFTrN environment.

(2) While existing DM methods are based on q-ROFTrNs, a CRITIC-based method tailored to the q-ROFTrN context still needs to be established.

(3) Although deep learning-based online learning assessment models show high accuracy, they require substantial computational resources [32]. New fuzzy DM methods need to improve efficiency in assessing complex and uncertain online learning engagement.

The q-ROFTrNs effectively represent complex scenario data adhering to trapezoidal variation patterns. Meanwhile, online learning engagement exhibits dynamic processes of rising, stabilizing, and declining. Therefore, the primary objective of this study is to develop an MADM method based on q-ROFTrNs. To achieve this, we first design a Yager operator for aggregating q-ROFTrNs by leveraging their advantages. On this basis, we develop an efficient MADM method for assessing complex and uncertain online learning engagement under a q-ROFTrN environment. To better accomplish the development of the MADM method for q-ROFTrNs, this paper proposes the q-Rung Orthopair Trapezoidal Fuzzy Yager Weighted Averaging (q-ROFTrNYWA) operator and MADM method based on q-ROFTrNs, and applies them simultaneously to online learning engagement assessment. Therefore, the main innovations of this study are summarized as follows:

(1) The q-ROFTrNYWA operator is developed, and its mathematical properties are established.

(2) An integrated MADM method q-Rung Orthogonal Trapezoidal Fuzzy Number Decision-Making (q-ROFTrNDM) is proposed based on q-ROFTrNs, which combines fuzzy distance, Yager operator, CRITIC method, and score function to achieve a comprehensive assessment of students' online learning engagement.

(3) The proposed q-ROFTrNDM is applied to assess online learning engagement by fusing the expert assessment values of multiple features (body posture, gaze, head posture, facial expressions). The comparison results confirm that the proposed q-ROFTrNDM is superior to the Principal Component Analysis method, the Expert Scoring Method, and the Factor Analysis method. Meanwhile, operator comparison analysis, sensitivity analysis, and time complexity analysis have all confirmed the stability and effectiveness of the q-ROFTrNDM method under various parameter settings.

The rest of this paper is organized as follows: Section 2 introduces the fundamental concepts required for this study, including q-ROFTrNYWA, score function, and distance formula under q-ROFTrNs. Section 3 details the q-ROFTrNYWA operator. Section 4 describes the q-ROFTrNDM. Section 5 provides experimental case studies and compares the performance of the assessment method based on the q-ROFTrNYWA operator with that of the q-ROFTrNDM method. Section 6 discusses the advantages and limitations of the q-ROFTrNDM, and gives future research directions. Section 7 concludes the paper.

2. Preliminaries

2.1 *Summary of notation and variables*

The mathematical symbols and variables mentioned in section 2 and 3 are all defined in Table 1. It is recommended that readers refer to this table at any time during their reading to clarify the meaning of the symbols.

Table 1. Summary of notation and variables

Abbreviation	Full term	Abbreviation	Full term
q	q-rung parameter	C_j	Importance index of feature j
y	Yager norm parameter	s_j	Standard deviation of feature j
$\widetilde{a}$	q-ROFTrN	q_{jk}	Correlation between features j and k
u	Membership degree	$Y^{(t)}$	Expert assessment matrix for group t
v	Non-membership degree	$D^{(t)}$	q-ROFTrN matrix for group t
π	Hesitation degree	$R^{(t)}$	Normalized decision matrix
$S(\widetilde{a})$	Score function	$\tilde{R}^{(t)}$	Aggregated engagement value for group t
$H(\widetilde{a})$	Accuracy function	$\widetilde{R}_{final}$	Final aggregated engagement value
$d\left(\widetilde{a}, \widetilde{b}\right)$	Distance between two q-ROFTrNs	m	Total number of images
$\oplus_Y$	Yager sum operator	n	Number of features
$\otimes_Y$	Yager product operator	T	Number of groups
w_i	Weight of feature j	k	Images per group

2.2 *Q-rung orthopair trapezoidal fuzzy number*

Definition 1 [33] Let X be the universe of discourse; $A = \{\langle x, u_A(x), v_A(x)\rangle | x \in X\}$ is q-ROFS on the universe X, the degree of membership $u_A : X \to (0, 1)$, the degree of non-membership $v_A : X \to (0, 1)$, and they are satisfied by the following formula (1).

$$0 \leq (u_A(x))^q + (v_A(x))^q \leq 1, \tag{1}$$

where $q \geq 1$, and the degree of hesitation $\pi_A(x)$ can be expressed as:

$$\pi_A(x) = \sqrt[q]{1 - (u_A(x))^q + (v_A(x))^q}(q \geq 1). \tag{2}$$

Definition 2 [34] Let $\widehat{a} = (a, b, c, d, u_a^{\sim}, v_a^{\sim})$ be a q-ROFTrN, and its membership function and non-membership function, respectively, satisfy formulas (3) and (4):

$$u_{\widehat{a}}(x) = \begin{cases} \dfrac{(x-a)u_a^{\sim}}{b-a}, \text{ if } (a \leq x < b) \\ u_a^{\sim}, \text{ if } (b \leq x \leq c) \\ \dfrac{(x-d)u_a^{\sim}}{d-c}, \text{ if } (c < x \leq d) \\ 0, \text{ if } (x < a, x > d) \end{cases} \tag{3}$$

$$v_{\widehat{a}}(x)=\begin{cases}\dfrac{(b-x+v_a^{\sim}(x-a))}{b-a},\ \text{if}\ (a\le x<b)\\[2ex] v_a^{\sim}\ ,\ \text{if}\ (b\le x\le c)\\[2ex] \dfrac{(x-c+v_a^{\sim}(d-x))}{d-c},\ \text{if}\ (c<x\le d)\\[2ex] 1,\ \text{if}\ (x<a,\ x>d).\end{cases} \tag{4}$$

Where $u_a^{\sim}$ is the maximum degree of membership of $\widehat{a}$ and $v_a^{\sim}$ is the minimum degree of non-membership of $\widehat{a}$, which satisfy $0\le u_{\widetilde{a}}{}^q+v_{\widetilde{a}}{}^q\le 1$ and $0\le u_{\widetilde{a}}{}^q\le 1,\ 0\le v_{\widetilde{a}}{}^q\le 1$.

Definition 3 [34] Let $\widetilde{a}=(a_1,\ a_2,\ a_3,\ a_4;\ u_{\widetilde{a}},\ v_{\widetilde{a}})$ and $\widetilde{b}=\left(b_1,\ b_2,\ b_3,\ b_4;\ u_{\widetilde{b}},\ v_{\widetilde{b}}\right)$ be two q-ROFTrN; $\gamma>0$ is random number; then, the following equations hold:

$$\widetilde{a}\oplus\widetilde{b}=\left(a_1+b_1,\ a_2+b_2,\ a_3+b_3,\ a_4+b_4;\ \sqrt[q]{u_{\widetilde{a}}{}^q+u_{\widetilde{b}}{}^q-u_{\widetilde{a}}{}^q u_{\widetilde{b}}{}^q},\ v_{\widetilde{a}}v_{\widetilde{b}}\right) \tag{5}$$

$$\widetilde{a}\otimes\widetilde{b}=\left(a_1b_1,\ a_2b_2,\ a_3b_3,\ a_4b_4;\ u_{\widetilde{a}}u_{\widetilde{b}},\ \sqrt[q]{v_{\widetilde{a}}{}^q+v_{\widetilde{b}}{}^q-v_{\widetilde{a}}{}^q v_{\widetilde{b}}{}^q}\right) \tag{6}$$

$$\gamma\widetilde{a}=\left(\gamma a_1,\ \gamma a_2,\ \gamma a_3,\ \gamma a_4;\ \sqrt[q]{1-(1-u_{\widetilde{a}}{}^q)^{\gamma}},\ v_{\widetilde{a}}{}^{\gamma}\right) \tag{7}$$

$$\widetilde{a}^{\gamma}=\left(a_1{}^{\gamma},\ a_2{}^{\gamma},\ a_3{}^{\gamma},\ a_4{}^{\gamma};\ u_{\widetilde{a}}{}^{\gamma},\ \sqrt[q]{1-(1-v_{\widetilde{a}}{}^q)^{\gamma}}\right). \tag{8}$$

For any two real numbers a and $b\in(0,\ 1)$, when $p=1$, the Yager operator reduces to the bounded sum and bounded product operators. As p approaches infinity, the Yager operator converges to the max and min operators. The "$\wedge$" denotes the minimum operator, which returns the smaller of the two values.

Definition 4 [35] The sum and product definitions of the Yager operator are as shown in formulas (9) and (10):

$$a\oplus_Y b=1\wedge\left(a^p+b^p\right)^{\frac{1}{p}},\ p\in[1,\ +\infty) \tag{9}$$

$$a\otimes_Y b=1-1\wedge\left((1-a)^p+(1-b)^p\right)^{\frac{1}{p}},\ p\in[1,\ +\infty). \tag{10}$$

2.3 *Fuzzy distance and score function formula*

In this paper, the decision matrix attribute weight solution requires calculating the distance [12] between q-ROFTrNs, while the DM method requires solving the score function of q-ROFTrNs. Inspired by the distance in Peng [36], this paper presents the distance definition of q-ROFTrNs, as shown in Definition 5.

Definition 5 [34] For any two $\widetilde{a}=(a_1,\ a_2,\ a_3,\ a_4;\ u_{\widetilde{a}},\ v_{\widetilde{a}})$ and $\widetilde{b}=\left(b_1,\ b_2,\ b_3,\ b_4;\ u_{\widetilde{b}},\ v_{\widetilde{b}}\right)$ q-ROFTrNs, where the distance is as shown in formula (11) $q\ge 1$.

$$d\left(\widetilde{a},\ \widetilde{b}\right)=\frac{1}{8}\left(\begin{array}{l}\left|a_1\sqrt[q]{1+u_{\widetilde{a}}^q-v_{\widetilde{a}}^q}-b_1\sqrt[q]{1+u_{\widetilde{b}}^q-v_{\widetilde{b}}^q}\right|+\\ \left|a_2\sqrt[q]{1+u_{\widetilde{a}}^q-v_{\widetilde{a}}^q}-b_2\sqrt[q]{1+u_{\widetilde{b}}^q-v_{\widetilde{b}}^q}\right|+\\ \left|a_3\sqrt[q]{1+u_{\widetilde{a}}^q-v_{\widetilde{a}}^q}-b_3\sqrt[q]{1+u_{\widetilde{b}}^q-v_{\widetilde{b}}^q}\right|+\\ \left|a_4\sqrt[q]{1+u_{\widetilde{a}}^q-v_{\widetilde{a}}^q}-b_4\sqrt[q]{1+u_{\widetilde{b}}^q-v_{\widetilde{b}}^q}\right|\end{array}\right). \tag{11}$$

Among them, $0\leq d\left(\widetilde{a},\ \widetilde{b}\right)\leq 1; d\left(\widetilde{a},\ \widetilde{b}\right)=d\left(\widetilde{b},\ \widetilde{a}\right); d\left(\widetilde{a},\ \widetilde{b}\right)=0$, if and only if $\widetilde{a}=\widetilde{b}$, if $\widetilde{a}\subseteq\widetilde{b}\subseteq\widetilde{c}$, then $d\left(\widetilde{a},\ \widetilde{b}\right)\leq d\left(\widetilde{a},\ \widetilde{c}\right)$ and $d\left(\widetilde{b},\ \widetilde{c}\right)\leq d\left(\widetilde{a},\ \widetilde{c}\right)$.

A variety of scoring functions have been proposed and are widely used for ranking intuitionistic fuzzy sets [37, 38]. These functions provide effective decision support for decision-makers. The score function and the accuracy function are presented as Definition 6 and Definition 7.

Definition 6 [34] Let $\widetilde{a}=\left(a_1,\ a_2,\ a_3,\ a_4;\ u_{\widetilde{a}},\ v_{\widetilde{a}}\right)$ is a q-ROFTrN, where $q\geq 1$. The score function S is defined as shown in formula (12).

$$S\left(\widetilde{a}\right)=\frac{\left(a_1+a_2+a_3+a_4\right)}{4}\times\left(u_{\widetilde{a}}{}^q-v_{\widetilde{a}}{}^q\right). \tag{12}$$

Definition 7 [34] Let $\widetilde{a}=\left(a_1,\ a_2,\ a_3,\ a_4;\ u_{\widetilde{a}},\ v_{\widetilde{a}}\right)$ is a q-ROFTrN, where $q\geq 1$. The definition of the accuracy function S is as shown in formula (13).

$$H\left(\widetilde{a}\right)=\frac{\left(a_1+a_2+a_3+a_4\right)}{4}\times\left(u_{\widetilde{a}}{}^q+v_{\widetilde{a}}{}^q\right). \tag{13}$$

Obviously, the accuracy function H reflects the degree of accuracy of $\widetilde{a}$ and $\widetilde{a}$ becomes more accurate as H increases. And the comparison method of q-ROFTrNs can be determined based on definitions 6 and 7.

Definition 8 [34] Suppose $\widetilde{a}=\left(a_1,\ a_2,\ a_3,\ a_4;\ u_{\widetilde{a}},\ v_{\widetilde{a}}\right)$ and $\widetilde{b}=\left(b_1,\ b_2,\ b_3,\ b_4;\ u_{\widetilde{a}},\ v_{\widetilde{a}}\right)$ are two q-ROFTrNs, where $q\geq 1$, $S\left(\widetilde{a}\right)$ and $S\left(\widetilde{b}\right)$ are the score values of $\widetilde{a}$ and $\widetilde{b}$ respectively, $H\left(\widetilde{a}\right)$ and $H\left(\widetilde{b}\right)$ are the accuracy values of $\widetilde{a}$ and $\widetilde{b}$ respectively. Then, the sorting method of q-ROFTrNs is introduced as follows:

(1) When $S\left(\widetilde{a}\right)>S\left(\widetilde{b}\right)$, then $\widetilde{a}>\widetilde{b}$; (2) When $S\left(\widetilde{a}\right)<S\left(\widetilde{b}\right)$, then $\widetilde{a}<\widetilde{b}$; (3) When $S\left(\widetilde{a}\right)=S\left(\widetilde{b}\right)$, if $H\left(\widetilde{a}\right)>H\left(\widetilde{b}\right)$ then $\widetilde{a}>\widetilde{b}$; if $H\left(\widetilde{a}\right)<H\left(\widetilde{b}\right)$ then $\widetilde{a}<\widetilde{b}$; if $H\left(\widetilde{a}\right)=H\left(\widetilde{b}\right)$, then $\widetilde{a}=\widetilde{b}$.

3. *Q*-rung orthopair trapezoidal fuzzy Yager operator

Inspired by the q-ROFTrN and the Yager operator, the rules for addition, multiplication, number multiplication, and exponentiation under the q-ROFTrN environment can be derived as shown in formulas (14)-(17).

Definition 9 Let $a=\left(a_1,\ a_2,\ a_3,\ a_4;\ u_1,\ v_1\right)$ sum $b=\left(b_1,\ b_2,\ b_3,\ b_4;\ u_2,\ v_2\right)$ are two q-ROFTrNs, where $q\geq 1$, $y\geq 1$, $\lambda\geq 0$, then the addition, multiplication, number multiplication, and power operation rules of the Yager operator for the q-ROFTrN are as shown in formulas (14) to (17).

$$a \oplus b = \left(\begin{array}{l} a_1 + b_1,\ a_2 + b_2,\ a_3 + b_3,\ a_4 + b_4, \\ \sqrt[q]{\min\left\{1,\ (u_1{}^{qy} + u_2{}^{qy})^{\frac{1}{y}}\right\}},\ \sqrt[q]{1 - \min\left\{1,\ ((1 - v_1{}^q)^y + (1 - v_2{}^q)^y)^{\frac{1}{y}}\right\}} \end{array} \right) \tag{14}$$

$$a \otimes b = \left(\begin{array}{l} a_1 b_1,\ a_2 b_2,\ a_3 b_3,\ a_4 b_4, \\ \sqrt[q]{1 - \min\left\{1,\ ((1 - u_1{}^q)^y + (1 - u_2{}^q)^y)^{\frac{1}{y}}\right\}},\ \sqrt[q]{\min\left\{1,\ (v_1{}^{qy} + v_2{}^{qy})^{\frac{1}{y}}\right\}} \end{array} \right) \tag{15}$$

$$\lambda a = \left(\lambda a_1,\ \lambda a_2,\ \lambda a_3,\ \lambda a_4,\ \sqrt[q]{\min\left\{1,\ (\lambda u^{qy})^{\frac{1}{y}}\right\}},\ \sqrt[q]{1 - \min\left\{1,\ (\lambda\,(1 - v^q)^y)^{\frac{1}{y}}\right\}} \right) \tag{16}$$

$$a^\lambda = \left(a_1^\lambda,\ a_2^\lambda,\ a_3^\lambda,\ a_4^\lambda,\ \sqrt[q]{1 - \min\left\{1,\ (\lambda\,(1 - u^q)^y)^{\frac{1}{y}}\right\}},\ \sqrt[q]{\min\left\{1,\ (\lambda v^{qy})^{\frac{1}{y}}\right\}} \right). \tag{17}$$

The rules of the Yager operator on q-ROFTrNs form the basis of the definition of the q-ROFTrNYWA operator.

Definition 10 Let $a_i = (a_{1i},\ a_{2i},\ a_{3i},\ a_{4i};\ u_{a_i},\ v_{a_i})\,(i = 1,\ 2,\ \ldots,\ n)$ is a set of q-ROFTrNs, where $y \geq 1,\ q \geq 1$, $w = (w_1,\ w_2,\ \ldots,\ w_n)^T$ is the weight vector. $w_i \geq 0,\ \sum_{i=1}^{n} w_i = 1$. Then the q-ROFTrNYWA operator is as shown in formula (18).

$$q\text{-ROFTrNYWA}\,(a_1,\ a_2,\ \ldots,\ a_n) = {}^{\oplus^n}_{i=1}\, w_i a_i. \tag{18}$$

Theorem 1 Let $a_i = (a_{1i},\ a_{2i},\ a_{3i},\ a_{4i};\ u_{a_i},\ v_{a_i})\,(i = 1,\ 2,\ \ldots,\ n)$ is a set of q-ROFTrNs, where $y \geq 1,\ q \geq 1$, and $w = (w_1,\ w_2,\ \ldots,\ w_n^T)$ is the weight vector. $w_i \geq 0,\ \sum_{i=1}^{n} w_i = 1$. Then the q-ROFTrNYWA operator calculates the expression as shown in formula (19), and the result is a q-ROFTrN.

$$\begin{aligned} & q\text{-ROFTrNYWA}\,(a_1,\ a_2,\ \ldots,\ a_n) \\ & = {}^{\oplus^n}_{i=1} w_i a_i \\ & = \left(\begin{array}{c} \sum_{i=1}^{n} w_i a_{i1},\ \sum_{i=1}^{n} w_i a_{i2},\ \sum_{i=1}^{n} w_i a_{i3},\ \sum_{i=1}^{n} w_i a_{i4}; \\ \sqrt[q]{\min\left\{1,\ \left(\sum_{i=1}^{n} w_i\,(u_{a_i}{}^q)^y\right)^{\frac{1}{y}}\right\}},\ \sqrt[q]{1 - \min\left\{1,\ \sum_{i=1}^{n} \left(w_i\,(1 - v_{a_i}{}^q)^y\right)^{\frac{1}{y}}\right\}} \end{array} \right). \end{aligned} \tag{19}$$

Proof. We prove this theorem using mathematical induction.

Step 1: For $n = 1$, when there is only one q-ROFTrN, the weight vector contains only $w_1 = 1$, as shown in formula (20):

$$
\begin{aligned}
&q\text{-ROFTrNYWA}\,(a_1)\\
&= w_1 a_1\\
&= \left(w_1 a_{11},\, w_1 a_{12},\, w_1 a_{13},\, w_1 a_{14};\, \sqrt[q]{\min\left\{1,\, \left(w_1\left(u_{a_1}^{q}\right)^{y}\right)^{\frac{1}{y}}\right\}},\, \sqrt[q]{1-\min\left\{1,\, \left(w_i\left(1-{v_{a_1}}^{q}\right)^{y}\right)^{\frac{1}{y}}\right\}}\right).
\end{aligned}
\tag{20}
$$

Since $w_1 = 1$, the calculation of membership and non-membership simplifies, as shown in formula (21):

$$
\sqrt[q]{\min\left\{1,\, \left(\left(u_{a_1}^{q}\right)^{y}\right)^{\frac{1}{y}}\right\}} = u_{a_1},\, \sqrt[q]{1-\min\left\{1,\, \left(\left(1-v_{a_1}^{q}\right)^{y}\right)^{\frac{1}{y}}\right\}} = v_{a_1}. \tag{21}
$$

Since $\left(\left(u_{a_i}^{q}\right)^{y}\right)^{\frac{1}{y}} = u_{a_1}^{q}$ and $\left(\left(1-v_{a_1}^{q}\right)^{y}\right)^{\frac{1}{y}} = 1-v_{a_1}^{q}$ and $u_{a_1}^{q} \le 1$, $\left(1-v_{a_1}^{q}\right) \le 1$, the min operators can be removed, as shown in formula (22):

$$
q\text{-ROFTrNYWA}\,(a_1) = \left(a_{11},\, a_{12},\, a_{13},\, a_{14};\, \sqrt[q]{u_{a_1}^{q}},\, \sqrt[q]{1-\left(1-{v_{a_1}}^{q}\right)}\right) = \left(a_{11},\, a_{12},\, a_{13},\, a_{14};\, u_{a_1}, v_{a_1}\right). \tag{22}
$$

Therefore, if the result is the same as the a_1 original, the result satisfies formula (19).

Step 2: For $n = 2$, let us consider two q-ROFTrNs a_1 and a_2 with weights w_1 and w_2 ($w_1 + w_2 = 1$). According to the Yager operation rules, the trapezoidal parameters are combined by linear weighting: $(w_1 a_{11} + w_2 a_{12},\, w_1 a_{21} + w_2 a_{22},\, w_1 a_{31} + w_2 a_{32},\, w_1 a_{41} + w_2 a_{42})$.

For the membership degree, as shown in formula (23):

$$
u = \sqrt[q]{\min\left\{1,\, \left(w_1\left({u_{a_1}}^{q}\right)^{y} + w_2\left({u_{a_2}}^{q}\right)^{y}\right)^{\frac{1}{y}}\right\}}. \tag{23}
$$

For the non-membership degree, as shown in formula (24):

$$
v = \sqrt[q]{1-\min\left\{1,\, \left(w_1\left(1-v_{a_1}^{q}\right)^{y} + w_2\left(1-v_{a_1}^{q}\right)^{y}\right)^{\frac{1}{y}}\right\}}. \tag{24}
$$

This shows the formula holds for $n = 2$.

Step 3: Suppose $n = k$, then for any k q-ROFTrN, a_1, ..., a_k. The result of the aggregation as shown in formula (25):

$$
q\text{-ROFTrNsYWA}\,(a_1,\, a_2,\, \ldots,\, a_k)
$$

$$= \left\{ \left(\sum_{i=1}^{k} w_i' a_{i1},\ \ldots,\ \sum_{i=1}^{k} w_i' a_{i4};\ \sqrt[q]{\min\{1,\ \left(\sum_{i=1}^{k} w_i' \left(u_{a_i}^q\right)^y \right)^{\frac{1}{y}}} \right);\ \sqrt[q]{1 - \min\left\{1,\ \left(\sum_{i=1}^{k} w_i' \left(1 - v_{a_i}^q\right)^y \right)^{\frac{1}{y}} \right\}} \right\}. \tag{25}$$

Where $w_i' = \dfrac{w_i}{\sum_{j=1}^{k} w_j}$ are normalized weights. For $n = k+1$, as shown in formula (26):

$$q\text{-ROFTrNYWA}(a_1,\ \ldots,\ a_{k+1}) = (\oplus_{i=1}^{k} w_i' a_i) \oplus w_{k+1} a_{k+1}. \tag{26}$$

Using the assumption and the operation rules for $n = 2$, we combine the aggregated result of the first k elements with the $(k+1)$th element. The trapezoidal parameters are linearly combined through weighted addition.

For the membership degree, we apply the Yager operation rule, as shown in formula (27):

$$u = \sqrt[q]{\min\left\{1,\ \left(\left(\min\left\{1,\ \left(\sum_{i=1}^{k} w_i'(u_{a_i}^q)^y\right)^{1/y}\right\}\right)^{qy} + \left(\min\left\{1,\ \left\{(w_{k+1}(u_{a_{k+1}}^q)^y)^{1/y}\right\}\right)^{qy}\right)^{1/y}\right\}}. \tag{27}$$

Since all weights sum to 1 and membership degrees are bounded, the inner min functions can be eliminated, as shown in formula (28):

$$u = \sqrt[q]{\min\left\{1,\ \left(\sum_{i=1}^{k} w_i'(u_{a_i}^q)^y + w_{k+1}(u_{a_{k+1}}^q)^y\right)^{1/y}\right\}}. \tag{28}$$

Substituting $w_i' = \dfrac{w_i}{\sum_{j=1}^{k} w_j}$ and noting that $\sum_{j=1}^{k} w_j = 1 - w_{k+1}$, as shown in formula (29):

$$u = \sqrt[q]{\min\left\{1,\ \left(\sum_{i=1}^{k+1} w_i(u_{a_i}^q)^y\right)^{1/y}\right\}}. \tag{29}$$

A similar derivation applies to the non-membership degree v, completing the inductive step. By mathematical induction, Theorem 1 holds for all positive integers n.

At the same time, the q-ROFTrNYWA operator satisfies permutation invariance, boundedness, monotonicity, and idempotency. These properties can be easily demonstrated by using formulas (14), (15), (16), and (17). The detailed proof process is omitted in this paper. □

4. *Q*-ROFTrNDM for online learning engagement assessment

In the specific assessment process of online learning engagement, student engagement is assessed based on the collected videos. The required image data is extracted from the original video using a sliding window. Then, the proposed

q-ROFTrNDM method is applied to assess the engagement level of each image, which integrates the CRITIC method with the q-ROFTrNYWA operator.

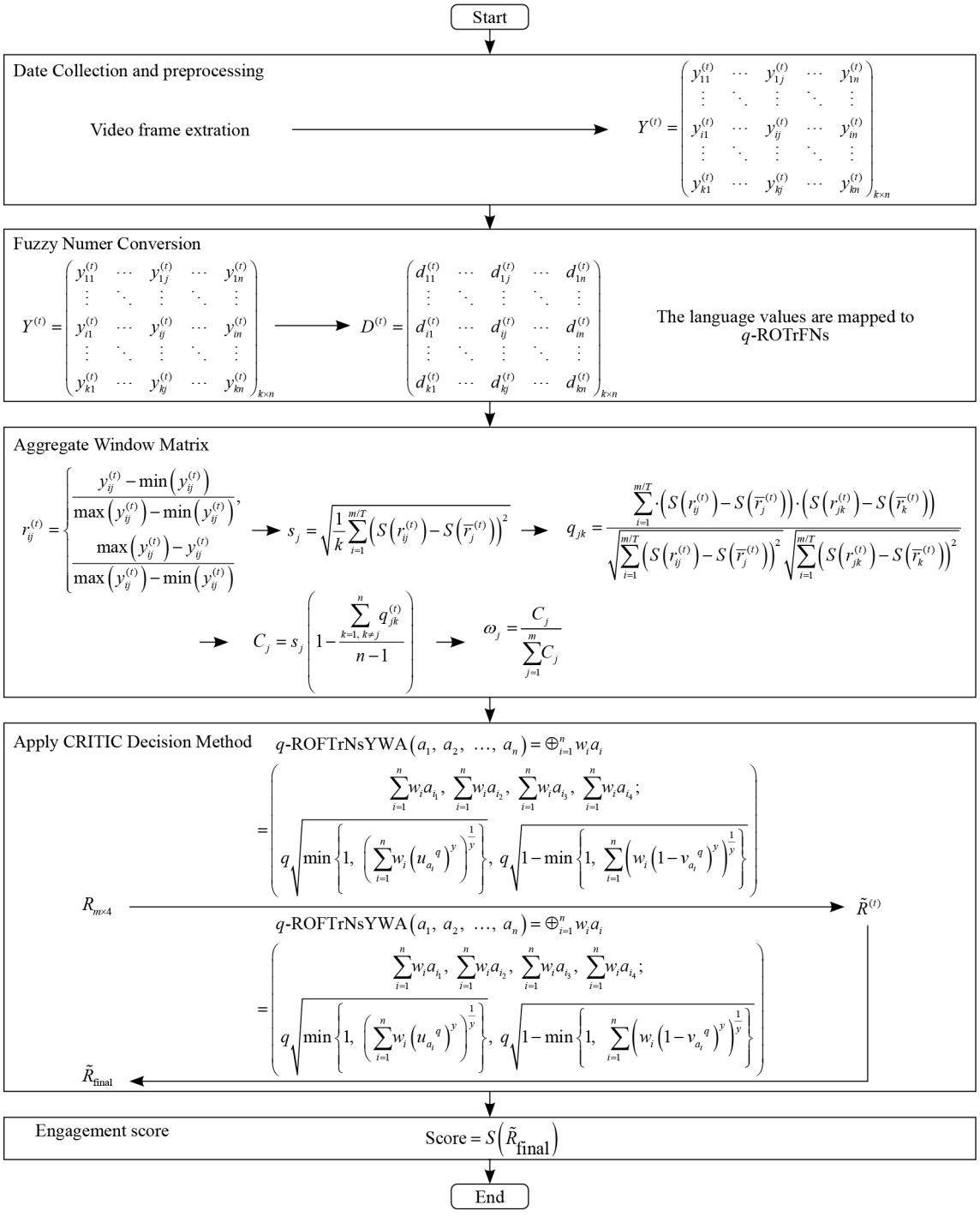

Figure 1. Engagement assessment process based on the CRITIC method

In the engagement assessment process for each student, m images are extracted from the collected videos, denoted as $P = \{p_1, p_2, \cdots, p_m\}$. Each image has n attributes: $C = \{c_1, c_2, \cdots, c_n\}$, and the attribute weight satisfies $\sum_1^n \omega_j =$

1, where $\omega_j \in [0,\ 1]$. The m images with n attributes are divided into T groups, obtaining an assessment matrix $Y^{(t)} = (y_{ij}^{(t)})_{k\times n}$, $(j = 1,\ \cdots,\ n,\ t = 1,\ \cdots,\ T,\ i = 1,\ \ldots,\ k$ and $k = m/T)$, as shown in formula (30).

The q-ROFTrNDM method includes two stages of information aggregation: (1) After the matrix $Y^{(t)}$ is transformed to $R^{(t)}$, the $R^{(t)}$ is aggregated to $\tilde{R}^{(t)}$ by the proposed q-ROFTrNYWA operator. (2) Then, the q-ROFTrNYWA operator is used to aggregate each row of $\tilde{R}^{(t)}$, and the result is $\tilde{R}_{\text{final}}$. The CRITIC method [39] provides an objective way to determine attribute weights by considering both the contrast intensity (standard deviation) of each feature and the conflict (correlation) between features. The overall assessment pipeline, illustrated in Figure 1, consists of the following steps.

Step 1: Data acquisition and preprocessing. (1) Collect online learning videos from online learners. (2) The collected video is split into individual images at a rate of one frame per second.

Step 2: Expert assessment. Based on the collected online learning videos, m collection points can be identified. An expert assigns rating levels to each feature and then classifies them into five grades: "very high", "high", "average", "poor", and "very poor". Finally, the $k \times n$-dimensional assessment decision matrix $Y^{(t)}$ is constructed. The assessment decision matrix $Y^{(t)}$ is shown as in formula (30).

$$Y^{(t)} = \begin{pmatrix} y_{11}^{(t)} & \cdots & y_{1j}^{(t)} & \cdots & y_{1n}^{(t)} \\ \vdots & \ddots & \vdots & \ddots & \vdots \\ y_{i1}^{(t)} & \cdots & y_{ij}^{(t)} & \cdots & y_{in}^{(t)} \\ \vdots & \ddots & \vdots & \ddots & \vdots \\ y_{k1}^{(t)} & \cdots & y_{kj}^{(t)} & \cdots & y_{kn}^{(t)} \end{pmatrix}_{k\times n}, \ i = 1,\ \ldots\ k,\ j = 1,\ \ldots,\ n,\ t = 1,\ \cdots,\ T. \tag{30}$$

Here, the elements $y_{ij}^{(t)}$ represent the level of engagement of the i^{th} collection point on the j^{th} feature within the t^{th} group.

Step 3: Fuzzy number conversion. The engagement language set data of different features is transformed into a q-ROFTrN matrix $D^{(t)}$, according to Table 2 [14], as shown in formula (31).

$$D^{(t)} = \begin{pmatrix} d_{11}^{(t)} & \cdots & d_{1j}^{(t)} & \cdots & d_{1n}^{(t)} \\ \vdots & \ddots & \vdots & \ddots & \vdots \\ d_{i1}^{(t)} & \cdots & d_{ij}^{(t)} & \cdots & d_{in}^{(t)} \\ \vdots & \ddots & \vdots & \ddots & \vdots \\ d_{k1}^{(t)} & \cdots & d_{kj}^{(t)} & \cdots & d_{kn}^{(t)} \end{pmatrix}_{k\times n}, \ i = 1,\ \ldots\ k,\ j = 1,\ \ldots,\ n,\ t = 1,\ \cdots,\ T. \tag{31}$$

Each element $d_{ij}^{(t)}$ is a q-ROFTrN corresponding to the assessment $y_{ij}^{(t)}$.

Table 2. Mapping relationships of language sets

Level of engagement	Engagement level	q-ROFTrNs
Extremely high	I	(0.80, 0.85, 0.90, 0.92; 0.87, 0.08)
Higher	II	(0.66, 0.70, 0.78, 0.81; 0.73, 0.20)
General	III	(0.45, 0.50, 0.55, 0.57; 0.50, 0.50)
Lower	IV	(0.30, 0.33, 0.38, 0.42; 0.32, 0.68)
Very low	V	(0.15, 0.20, 0.23, 0.28; 0.15, 0.80)

Step 4: Normalization. To eliminate the influence of different dimensions, normalize the matrix $Y^{(t)}$, where benefit-type features (the larger, the better) can be normalized with max-minimum; for cost-type features (the smaller, the better), reverse processing is possible, and the matrix $Y^{(t)}$ is normalized as $R^{(t)}$, where $r_{ij}^{(t)}$ is the normalized value of $y_{ij}^{(t)}$, as shown in formula (32), where $\min(y_{ij}^{(t)}) = \min\{y_{1j}^{(t)}, \ldots, y_{kj}^{(t)}\}$, $\max(y_{ij}^{(t)}) = \max\{y_{1j}^{(t)}, y_{2j}^{(t)}, \ldots, y_{kj}^{(t)}\}$, $i = 1, \ldots k,\ j = 1, \ldots, n,\ t = 1, \cdots, T$.

$$r_{ij}^{(t)} = \begin{cases} \dfrac{y_{ij}^{(t)} - \min(y_{ij}^{(t)})}{\max(y_{ij}^{(t)}) - \min(y_{ij}^{(t)})},\ \text{benefit} - \text{type} \\ \\ \dfrac{\max(y_{ij}^{(t)}) - y_{ij}^{(t)}}{\max(y_{ij}^{(t)}) - \min(y_{ij}^{(t)})},\ \text{cost} - \text{type} \end{cases}. \tag{32}$$

Step 5: Derive the attribute weight.

Step 5.1: Calculate the standard deviation for each feature. Standard deviation is an important measure of the degree of fluctuation of a feature. The standard deviation s_j of each feature is shown in formula (33).

$$s_j = \sqrt{\frac{1}{k}\sum_{i=1}^{m/T}\left(S(r_{ij}^{(t)}) - S(\bar{r}_j^{(t)})\right)^2}\ \ i = 1, \ldots k,\ j = 1, \ldots, n,\ t = 1, \cdots, T. \tag{33}$$

In formula (33), $S\left(r_{ij}^{(t)}\right)$ is the score of the i^{th} collection point on the j^{th} feature, $S(\bar{r}_j^{(t)})$ represents the mean score of all collection points for the j^{th} feature within the t^{th} group, m represents the number of samples, and $\bar{r}_j^{(t)}$ represents the average of the j^{th} feature.

Step 5.2: Calculate the correlation coefficient between features. The Pearson correlation coefficient is used to represent the relationship between features, as shown in formula (34), where $i = 1, \ldots k$, $k = \dfrac{m}{T}$; $j = 1, \ldots, n$, $t = 1, \ldots, T$, and the q_{jk} indicates the degree of correlation between two features.

$$q_{jk} = \frac{\sum_{i=1}^{m/T}\left(S(r_{ij}^{(t)}) - S(\bar{r}_j^{(t)})\right)\left(S(r_{jk}^{(t)}) - S(\bar{r}_k^{(t)})\right)}{\sqrt{\sum_{i=1}^{m/T}\left(S(r_{ij}^{(t)}) - S(\bar{r}_j^{(t)})\right)^2}\sqrt{\sum_{i=1}^{m/T}\left(S(r_{jk}^{(t)}) - S(\bar{r}_k^{(t)})\right)^2}}. \tag{34}$$

In formula (34), $S\left(r_{jk}^{(t)}\right)$ is the score value of the j^{th} collection point on the k^{th} feature within the t^{th} group, and $S(\bar{r}_k^{(t)})$ represents the mean score of all collection points for the k^{th} feature.

Step 5.3: Calculate the importance index for each feature. The CRITIC method assumes that the importance of a feature is determined by its standard deviation and non-correlation with other features. It calculates the importance index C_j for each feature as shown in formula (35).

$$C_j = s_j \left(1 - \frac{\sum_{k=1,\, k\neq j}^{n} q_{jk}^{(t)}}{n-1} \right). \tag{35}$$

In formula (35), n represents the number of features. The formula reflects the volatility of the feature itself and its independence from other features.

Step 5.4: Calculate the weight of the feature. Normalize the importance index of all features to obtain the weight of each feature ω_j as shown in formula (36).

$$\omega_j = \frac{C_j}{\sum_{j=1}^{m} C_j}. \tag{36}$$

Step 6: Feature aggregation. The q-ROFTrNYWA operator is used to aggregate the engagement assessment values as shown in formula (37), where $i = 1, \ldots, k,\ j = 1, \ldots, n,\ t = 1, \ldots, T$.

$$\tilde{R}^{(t)} = q\text{-ROFTrNYWA}\left(\tilde{r}_{ij}^{(t)}, \tilde{r}_{ij}^{(t)}, \tilde{r}_{ij}^{(t)}, \ldots, \tilde{r}_{ij}^{(t)} \right). \tag{37}$$

In formula (37), $\tilde{R}^{(t)}$ represents the overall engagement assessment value of the t^{th} group, and $\tilde{r}_{ij}^{(t)}$ $(i = 1, \ldots, k)$, represents the engagement assessment values of the k images within the t^{th} group.

Step 7: Engagement assessment. Obtain assessment values $\left(\left(\tilde{R}^{(1)}, \tilde{R}^{(2)} \right), \ldots, \tilde{R}^{(T)} \right)$ according to Step 6. The q-ROFTrNYWA operator is used to aggregate $\tilde{R}^{(1)}, \tilde{R}^{(2)}, \ldots, \tilde{R}^{(T)}$, as shown in formula (38).

$$\tilde{R}_{\text{final}} = q\text{-ROFTrNYWA}\left(\tilde{R}^{(1)}, \tilde{R}^{(2)}, \ldots, \tilde{R}^{(T)} \right) \tag{38}$$

Step 8: Engagement score. Calculate the final engagement score using formula (39):

$$\text{Score} = S\left(\widetilde{R}_{\text{final}} \right). \tag{39}$$

Where $S\left(\widetilde{R}_{\text{final}} \right)$ is the scoring function defined in Definition 6 with a value range of $[-1, 1]$. A higher value indicates stronger engagement.

5. Experimental cases

5.1 *Case background*

In the context of online classes for students and teachers, teachers face a major problem in tracking students' engagement levels. Given that students' engagement is closely related to online learning outcomes, and that video data

needs to be processed on students' devices to protect privacy. To build a fast and accurate engagement assessment model, a multi-feature recognition method that integrates body posture, gaze direction, head posture, and facial expressions can provide more accurate results compared to single-feature recognition. Students' online learning engagement can be measured in various ways, such as self-assessment, expert assessment, and scale scoring, all of which are valuable feedback resources. Moreover, the assessment results provide data support for teachers to help optimize teaching methods and improve students' learning outcomes. In addition, the assessment results of students' online learning can provide a scientific reference for educational assessment and policy-making, promoting the development and reform of the education sector. The multi-feature fuzzy comprehensive assessment methods include four features, as shown below.

(1) Body posture (c_1). Students' posture serves as an effective indicator of learning engagement [40]. Maintaining a body posture with a small range of motion is associated with higher engagement.

(2) Gaze (c_2). Eye movement trajectories are key parameters for measuring engagement [41]. Using non-contact eye-tracking technology can precisely record the duration and movement path of the fixation point in the screen area, effectively identifying engagement-shifting behavior.

(3) Head posture (c_3). Head orientation changes reflect sustained engagement characteristics [42]. Early signs of distraction can be detected by monitoring the deflection angle of the head in real time through a three-dimensional pose analysis algorithm, combined with comparative analysis of benchmark learning poses.

(4) Facial expressions (c_4). Significant correlation exists between micro-expressions and cognitive engagement [43]. Using facial expression recognition technology to analyze subtle changes in the eyebrow and eye regions and mouth muscles can construct a quantitative relationship between emotional state and learning engagement.

5.2 *Case study of q-ROFTrNDM for assessing engagement*

In this experiment, all data collection procedures strictly adhered to established ethical guidelines. Explicit informed consent was obtained from the participants, clearly outlining the purpose of data collection and that the data would only be used for academic research. To strictly protect privacy, mosaics were added to all participants' video images during the data preprocessing process. During implementation, 20 students from the research team were invited to record their online learning process, with each student's total duration being 10 minutes. 600 images are extracted every second, resulting in $m = 600$, $n = 4$, $T = 60$, $k = 10$. In this case study, five students (stu1, stu2, stu3, stu4, stu5) were randomly selected from a group of 20 students for the implementation of the decision-making method. The engagement assessment method of q-ROFTrNDM includes 8 steps, and the case is implemented as follows.

Step 1: Data preprocessing.

The data collection includes two processes. (1) Among the 20 students recorded during the online learning process, five students (stu 1, stu 2, stu 3, stu 4, stu 5) were randomly selected, with a total duration of 10 minutes for each student. (2) Images are extracted at a rate of 1 frame per second, resulting in a total of 600 frames. That is, using video editing software, single images of each student are captured from the video at a rate of one frame per second. As shown in Figure 2, 10 images captured by the student stu1 within the first 10 seconds are presented.

Figure 2. 10 images of the student stu1 within 10 seconds

Step 2: Expert assessment.

An expert is invited to assess the images extracted at one frame per second from the video and label the results based on four features of each image. And the assessment value of stu1 is presented in a matrix $Y^{(t)}$ $(t = 1)$. The engagement level of 10 images from stu1 is shown in Table 3, p_1 to p_{10} represent the number of images.

Table 3. Engagement levels of features across 10 images of student stu1

	c_1	c_2	c_3	c_4
p_1	II	V	IV	V
p_2	III	IV	V	V
p_3	IV	V	V	IV
p_4	III	V	V	V
p_5	III	V	V	III
p_6	II	V	V	V
p_7	III	V	V	IV
p_8	III	V	IV	V
p_9	III	V	V	V
p_{10}	III	V	V	V

The assessment grades include "very high", "high", "average", "poor", and "very poor", represented by V, IV, III, II, and I, respectively. This method can more accurately reflect the changes in students' engagement throughout the online learning process, providing strong support for personalized teaching and learning strategy adjustments.

Step 3: Fuzzy number conversion.

According to the fuzzy set mapping relationship in Table 2 and formula (31), the matrix $Y^{(t)}$ $(t = 1)$ is a transformed matrix $D^{(t)}$, as shown in Table 4. And the p_1 to p_{10} represent the number of images.

Table 4. The q-ROFTrNs matrix transformed from the engagement level of 10 images

Index	c_1	c_2	c_3	c_4
p_1	(0.66, 0.70, 0.78, 0.81; 0.73, 0.20)	(0.15, 0.20, 0.23, 0.28; 0.15, 0.80)	(0.30, 0.33, 0.38, 0.42; 0.32, 0.68)	(0.15, 0.20, 0.23, 0.28; 0.15, 0.80)
p_2	(0.45, 0.50, 0.55, 0.57; 0.50, 0.50)	(0.30, 0.33, 0.38, 0.42; 0.32, 0.68)	(0.15, 0.20, 0.23, 0.28; 0.15, 0.80)	(0.15, 0.20, 0.23, 0.28; 0.15, 0.80)
p_3	(0.30, 0.33, 0.38, 0.42; 0.32, 0.68)	(0.15, 0.20, 0.23, 0.28; 0.15, 0.80)	(0.15, 0.20, 0.23, 0.28; 0.15, 0.80)	(0.30, 0.33, 0.38, 0.42; 0.32, 0.68)
p_4	(0.45, 0.50, 0.55, 0.57; 0.50, 0.50)	(0.15, 0.20, 0.23, 0.28; 0.15, 0.80)	(0.15, 0.20, 0.23, 0.28; 0.15, 0.80)	(0.15, 0.20, 0.23, 0.28; 0.15, 0.80)
p_5	(0.45, 0.50, 0.55, 0.57; 0.50, 0.50)	(0.15, 0.20, 0.23, 0.28; 0.15, 0.80)	(0.15, 0.20, 0.23, 0.28; 0.15, 0.80)	(0.45, 0.50, 0.55, 0.57; 0.50, 0.50)
p_6	(0.66.0.70.0.78.0.81; 0.73.0.20)	(0.15, 0.20, 0.23, 0.28; 0.15, 0.80)	(0.15, 0.20, 0.23, 0.28; 0.15, 0.80)	(0.15, 0.20, 0.23, 0.28; 0.15, 0.80)
p_7	(0.45, 0.50, 0.55, 0.57; 0.50, 0.50)	(0.15, 0.20, 0.23, 0.28; 0.15, 0.80)	(0.15, 0.20, 0.23, 0.28; 0.15, 0.80)	(0.30, 0.33, 0.38, 0.42; 0.32, 0.68)
p_8	(0.45, 0.50, 0.55, 0.57; 0.50, 0.50)	(0.15, 0.20, 0.23, 0.28; 0.15, 0.80)	(0.30, 0.33, 0.38, 0.42; 0.32, 0.68)	(0.15, 0.20, 0.23, 0.28; 0.15, 0.80)
p_9	(0.45, 0.50, 0.55, 0.57; 0.50, 0.50)	(0.15, 0.20, 0.23, 0.28; 0.15, 0.80)	(0.15, 0.20, 0.23, 0.28; 0.15, 0.80)	(0.15, 0.20, 0.23, 0.28; 0.15, 0.80)
p_{10}	(0.45, 0.50, 0.55, 0.57; 0.50, 0.50)	(0.15, 0.20, 0.23, 0.28; 0.15, 0.80)	(0.15, 0.20, 0.23, 0.28; 0.15, 0.80)	(0.15, 0.20, 0.23, 0.28; 0.15, 0.80)

Step 4: Normalize the data.

To eliminate the dimensional differences between features, the matrix $Y^{(t)}$ is transformed into a standardized matrix $R^{(t)}$ according to formula (32), as shown in Table 5, where p_1 to p_{10} represent the number of images.

Table 5. The normalized decision matrix reflected by the first 10 images of student stu1

Index	c_1	c_2	c_3	c_4
p_1	1.00	0.25	1.00	0.75
p_2	1.00	0.75	1.00	1.00
p_3	1.00	1.00	1.00	0.75
p_4	0.67	1.00	1.00	1.00
p_5	1.00	1.00	1.00	1.00
p_6	0.67	1.00	1.00	1.00
p_7	0.67	1.00	1.00	1.00
p_8	0.67	1.00	1.00	1.00
p_9	0.67	1.00	1.00	1.00
p_{10}	1.00	0.25	1.00	0.75

Step 5: Calculate attribute weights.

Step 5.1: Calculate the standard deviation. Calculate the standard deviation for each feature s_j to measure the degree of dispersion of the data distribution, and calculate the standard deviation for $R^{(t)}$ according to formula (33). As shown in Table 6, the stu1 presents the first student, s_1 to s_4 respectively represent the standard deviations of the four features of stu1.

Table 6. Standard deviations of four features

Index	s_1	s_2	s_3	s_4
stu1	0.344	0.210	0.288	0.287

Step 5.2: Calculate the correlation coefficient between features. According to formula (34), the correlation coefficient $q_{jk}^{(t)}$ of the stu1 is calculated. The correlation coefficient matrix is shown in Table 7.

Table 7. Correlation coefficients among four features

Index	s_1	s_2	s_3	s_4
c_1	1.00	0.53	0.59	0.62
c_2	0.53	1.00	0.8	0.79
c_3	0.59	0.80	1.00	0.89
c_4	0.62	0.79	0.89	1.00

Step 5.3: Calculate the importance index. Combine the standard deviation s_j with the correlation coefficient $q_{jk}^{(t)}$ to calculate the importance index C_j for each feature. The importance index is calculated according to formula (35), as shown in Table 8. stu1 represents the first student, and C_1 to C_4 represent the importance indices of the four features of stu1.

Table 8. Importance Index of the four features

Index	C_1	C_2	C_3	C_4
stu1	0.290	0.176	0.235	0.237

Step 5.4: Calculate the feature weights. Finally, the importance index of all features is normalized to obtain the weight of each feature ω_j, according to formula (36). The calculated feature weights are shown in Table 9. ω_1 to ω_4 respectively represent the four different feature weights for student stu1.

Table 9. Feature weights for four features of student stu1

Index	ω_1	ω_2	ω_3	ω_4
stu1	0.3094	0.1881	0.2502	0.2523

As we can see from Table 8, the body posture (C_1) has the greatest impact on the stu1 engagement assessment (weight 0.3094). At the same time, gaze (C_2) contributes the least (0.1881), indicating the difference in feature weights among different individuals.

Step 6: 10-second level engagement feature aggregation.

The 600 images of stu1 are divided into 60 groups, resulting in $m = 600$, $n = 4$, $T = 60$, $k = 10$. The q-ROFTrNYWA operator is used to calculate the engagement assessment values by formula (37). For the student stu1, the engagement assessment value of the first group is calculated by the q-ROFTrNYWA operator, and the result is

$$\tilde{R}^{(1)} = (0.441,\ 0.486,\ 0.539,\ 0.564;\ 0.444,\ 0.558)$$

When $t = 1, \ldots, 60$, we can obtain 60 engagement assessment values of student stu1, and the assessment values are shown in Table 10.

Step 7: Engagement feature aggregation.

The q-ROFTrNYWA operator is used to aggregate the $\tilde{R}^{(t)}$ $(t = 1, \ldots, 60)$ according to formula (38). Then, the engagement assessment value of stu1 is as follows.

$$\tilde{R}_{\text{final}} = (0.64,\ 0.69,\ 0.74,\ 0.77;\ 0.72,\ 0.31)$$

Based on steps 1-7, the engagement assessment values of the other students (stu2, stu3, stu4, and stu5) are obtained, and the online learning engagement assessment values of five students are shown in Table 11.

The results suggest that the q-ROFTrNYWA operator outperforms conventional operators in dynamic weight allocation and multi-feature fusion.

Table 10. The engagement assessment value for the student stu1

Index	value	Index	value	Index	value
$\tilde{R}^{(1)}$	(0.441, 0.486, 0.539, 0.564; 0.444, 0.558)	$\tilde{R}^{(21)}$	(0.489, 0.533, 0.593, 0.622; 0.461, 0.549)	$\tilde{R}^{(41)}$	(0.468, 0.509, 0.568, 0.597; 0.463, 0.540)
$\tilde{R}^{(2)}$	(0.555, 0.600, 0.665, 0.690; 0.482, 0.522)	$\tilde{R}^{(22)}$	(0.504, 0.550, 0.610, 0.637; 0.461, 0.549)	$\tilde{R}^{(42)}$	(0.453, 0.492, 0.551, 0.582; 0.463, 0.540)
$\tilde{R}^{(3)}$	(0.501, 0.543, 0.607, 0.641; 0.469, 0.549)	$\tilde{R}^{(23)}$	(0.411, 0.452, 0.505, 0.534; 0.444, 0.558)	$\tilde{R}^{(43)}$	(0.483, 0.526, 0.585, 0.612; 0.463, 0.540)
$\tilde{R}^{(4)}$	(0.468, 0.513, 0.570, 0.598; 0.452, 0.558)	$\tilde{R}^{(24)}$	(0.408, 0.453, 0.506, 0.540; 0.427, 0.591)	$\tilde{R}^{(44)}$	(0.285, 0.329, 0.371, 0.409; 0.381, 0.630)
$\tilde{R}^{5}$	(0.366, 0.401, 0.454, 0.489; 0.444, 0.558)	$\tilde{R}^{(25)}$	(0.366, 0.405, 0.456, 0.490; 0.431, 0.575)	$\tilde{R}^{(45)}$	(0.165, 0.213, 0.245, 0.294; 0.303, 0.702)
$\tilde{R}^{(6)}$	(0.375, 0.419, 0.467, 0.496; 0.421, 0.583)	$\tilde{R}^{(26)}$	(0.360, 0.402, 0.450, 0.481; 0.421, 0.583)	$\tilde{R}^{(46)}$	(0.195, 0.239, 0.275, 0.322; 0.336, 0.674)
$\tilde{R}^{(7)}$	(0.459, 0.499, 0.559, 0.592; 0.461, 0.549)	$\tilde{R}^{(27)}$	(0.447, 0.489, 0.545, 0.573; 0.454, 0.549)	$\tilde{R}^{(47)}$	(0.165, 0.213, 0.245, 0.294; 0.303, 0.702)
$\tilde{R}^{(8)}$	(0.540, 0.583, 0.648, 0.675; 0.482, 0.522)	$\tilde{R}^{(28)}$	(0.423, 0.462, 0.519, 0.553; 0.452, 0.558)	$\tilde{R}^{(48)}$	(0.165, 0.213, 0.245, 0.294; 0.303, 0.702)
$\tilde{R}^{(9)}$	(0.342, 0.386, 0.434, 0.472; 0.404, 0.615)	$\tilde{R}^{(29)}$	(0.453, 0.492, 0.551, 0.582; 0.463, 0.540)	$\tilde{R}^{(49)}$	(0.150, 0.200, 0.230, 0.280; 0.285, 0.715)
$\tilde{R}^{(10)}$	(0.432, 0.476, 0.530, 0.559; 0.442, 0.566)	$\tilde{R}^{(30)}$	(0.462, 0.506, 0.562, 0.588; 0.454, 0.549)	$\tilde{R}^{(50)}$	(0.150, 0.200, 0.230, 0.280; 0.285, 0.715)
$\tilde{R}^{(11)}$	(0.351, 0.392, 0.441, 0.476; 0.419, 0.591)	$\tilde{R}^{(31)}$	(0.447, 0.493, 0.547, 0.574; 0.442, 0.566)	$\tilde{R}^{(51)}$	(0.165, 0.213, 0.245, 0.294; 0.303, 0.702)
$\tilde{R}^{(12)}$	(0.300, 0.342, 0.386, 0.423; 0.395, 0.615)	$\tilde{R}^{(32)}$	(0.336, 0.379, 0.426, 0.462; 0.406, 0.607)	$\tilde{R}^{(52)}$	(0.255, 0.295, 0.337, 0.379; 0.381, 0.630)
$\tilde{R}^{(13)}$	(0.423, 0.466, 0.521, 0.554; 0.440, 0.575)	$\tilde{R}^{(33)}$	(0.498, 0.543, 0.602, 0.627; 0.463, 0.540)	$\tilde{R}^{(53)}$	(0.483, 0.526, 0.585, 0.612; 0.463, 0.540)
$\tilde{R}^{(14)}$	(0.639, 0.680, 0.757, 0.786; 0.518, 0.483)	$\tilde{R}^{(34)}$	(0.540, 0.583, 0.648, 0.675; 0.482, 0.522)	$\tilde{R}^{(54)}$	(0.519, 0.563, 0.625, 0.651; 0.473, 0.531)
$\tilde{R}^{(15)}$	(0.534, 0.580, 0.642, 0.666; 0.473, 0.531)	$\tilde{R}^{(35)}$	(0.525, 0.566, 0.631, 0.660; 0.482, 0.522)	$\tilde{R}^{(55)}$	(0.435, 0.483, 0.533, 0.555; 0.433, 0.567)
$\tilde{R}^{(16)}$	(0.540, 0.583, 0.648, 0.675; 0.482, 0.522)	$\tilde{R}^{(36)}$	(0.426, 0.469, 0.522, 0.549; 0.444, 0.558)	$\tilde{R}^{(56)}$	(0.504, 0.546, 0.608, 0.636; 0.473, 0.531)
$\tilde{R}^{(17)}$	(0.492, 0.540, 0.596, 0.618; 0.454, 0.549)	$\tilde{R}^{(37)}$	(0.456, 0.503, 0.556, 0.579; 0.444, 0.558)	$\tilde{R}^{(57)}$	(0.561, 0.603, 0.671, 0.699; 0.491, 0.513)
$\tilde{R}^{(18)}$	(0.597, 0.640, 0.711, 0.738; 0.500, 0.503)	$\tilde{R}^{(38)}$	(0.411, 0.456, 0.507, 0.535; 0.431, 0.575)	$\tilde{R}^{(58)}$	(0.561, 0.603, 0.671, 0.699; 0.491, 0.513)
$\tilde{R}^{(19)}$	(0.576, 0.620, 0.688, 0.714; 0.491, 0.513)	$\tilde{R}^{(39)}$	(0.498, 0.543, 0.602, 0.627; 0.463, 0.540)	$\tilde{R}^{(59)}$	(0.462, 0.506, 0.562, 0.588; 0.454, 0.549)
$\tilde{R}^{(20)}$	(0.555, 0.600, 0.665, 0.690; 0.482, 0.522)	$\tilde{R}^{(40)}$	(0.330, 0.372, 0.418, 0.452; 0.408, 0.599)	$\tilde{R}^{(60)}$	(0.597, 0.640, 0.711, 0.738; 0.500, 0.503)

Table 11. Final engagement aggregation result of five students

Index	stu1	stu2	stu3	stu4	stu5
$\tilde{R}_{\text{final}}$	(0.64, 0.69, 0.74, 0.77; 0.72, 0.31)	(0.63, 0.68, 0.74, 0.76; 0.71, 0.32)	(0.65, 0.69, 0.75, 0.77; 0.73, 0.32)	(0.63, 0.68, 0.73, 0.76; 0.71, 0.34)	(0.54, 0.58, 0.64, 0.66; 0.63, 0.46)

Step 8: Engagement score.

Based on Table 11 and using formula (39), the engagement assessment scores of five students are obtained, as shown in Table 12.

Table 12. Final engagement score of five students

Index	stu1	stu2	stu3	stu4	stu5
$S\left(\widetilde{R}_{\text{final}}\right)$	0.50	0.49	0.51	0.49	0.36

From Table 12, it can be seen that the score for stu5 is 0.36, indicating low engagement, and the score for stu3 is 0.51, indicating average engagement. This is consistent with the expert's assessment of the engagement levels of stu5 and stu3. Therefore, the assessment results obtained by the q-ROFTrNDM method are basically consistent with the expert's assessment results.

From the implementation results of the case, the q-ROFTrNDM model can effectively assess online learning engagement based on expert language assessment values. It can be seen that teachers can discern changes in students' engagement levels based on this and implement targeted teaching strategies accordingly, such as adjusting the teaching pace and providing personalized learning support. From the perspective of educational management, the proposed method can be used to assess the effectiveness of online learning and assist educators in improving teaching quality.

5.3 *Sensitivity coefficient analysis*

To further verify the feasibility of the fuzzy decision assessment method proposed in this paper, this section mainly analyzes the influence of different parameters of q-ROFTrNDM on the assessment results. Based on the case in section 5.2, when $y = 2$ and q vary from 2 to 9, respectively, the engagement assessment values are recalculated multiple times, and the score assessment results of each student under different q values are shown in Figure 3. As shown in the figure, when q values change from 2 to 9, the rankings of students remain unchanged, which indicates the stability of the proposed q-ROFTrNDM method.

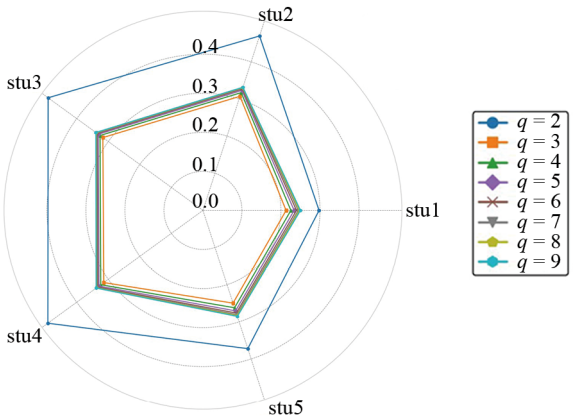

Figure 3. Score assessment results for each student at different q values

Similarly, based on the case study in section 5.2, when $q = 2$ and y vary from 2 to 9, the engagement assessment values are recalculated. The assessment scores for each student under different y values are shown in Figure 4. As observed from Figure 4, as y vary from 2 to 9, the ranking order of students remains consistent, further verifying the stability of the proposed q-ROFTrNDM method.

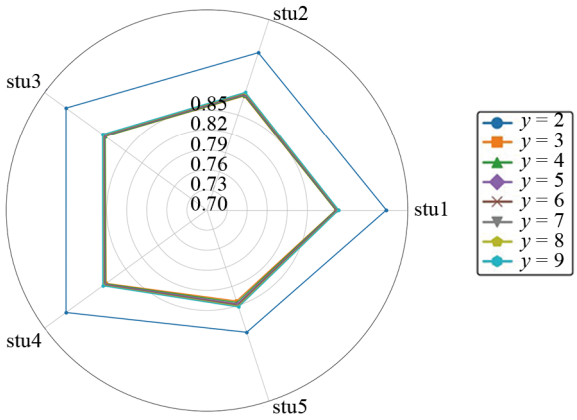

Figure 4. Score assessment results for each student under different y values

5.4 *Comparative analysis of q-ROFTrNYWA operator*

To further verify the feasibility and effectiveness of the engagement assessment method. In this section, we utilize assessment data from 5 students to compute their online learning engagement at each given moment. Initially, we employ formula (19) to aggregate the fuzzy scores of each student from their previous moments to the current one. We then compare these scores with the ranges of ([0.66, 0.70, 0.78, 0.81; 0.73, 0.20], [0.45, 0.50, 0.55, 0.57; 0.50, 0.50]). If the current score exceeds these ranges, we classify the student as being focused at that moment, denoted as 1. Otherwise, it is classified as 0. Subsequently, we compute the average engagement level of the 5 students at each moment. The q-ROFTrNYWA operator is compared with the q-ROFWAA (WAA) [44], q-ROFWA (WA) [45], q-ROFWHM (HM) [46], q-ROFWSS (WSS) [47], and q-ROFWH (WH) [48] operators.

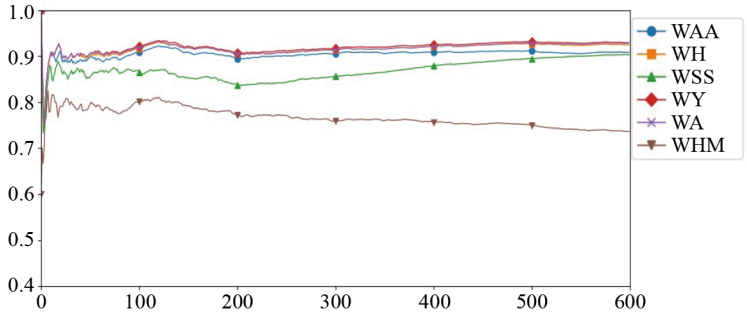

Figure 5. The results of the different operators

The advantages and characteristics of the q-ROFTrNYWA operator in the assessment process can be visually demonstrated. To ensure the scientific and effective nature of the operator comparative analysis, the parameter q of all operators is uniformly set to 2. Meanwhile, in q-ROFWY, $y = 2$; in q-ROFWHM, $r = s = 1$, in q-ROFWSS, $z = 5$. Other operators have no additional parameters. The performance of the q-ROFTrNYWA operator in the engagement assessment methods is assessed more accurately, as shown in Figure 5. The horizontal axis represents time points, and the vertical axis represents the level of online learning engagement. The higher the score, the stronger the online learning engagement. Table 13 shows the classroom engagement scores at time points 0, 100, 200, 300, 400, 500, and 600.

Table 13. Online learning engagement scores for each operator at different time points

	0	100	200	300	400	500	600
WAA	1.0000	0.9100	0.8970	0.9053	0.9085	0.9112	0.9080
WH	1.0000	0.9180	0.9060	0.9133	0.9205	0.9268	0.9243
WSS	1.0000	0.8680	0.8390	0.8560	0.8785	0.8948	0.9027
WA	1.0000	0.9200	0.9060	0.9133	0.9205	0.9284	0.9277
WHM	0.6000	0.8020	0.7740	0.7587	0.7570	0.7504	0.7363
WY (Proposed)	1.0000	0.9220	0.9090	0.9167	0.9240	0.9312	0.9290

From Figure 5 and Table 13, it can be seen that as time goes by, the online learning engagement scores of the WAA, WA, WHM, WSS, and WH operators converge after 200 frames. The online learning assessment of the WY operator always remains the highest at convergence, reaching above 0.929, which is generally higher than that of other operators. Moreover, before 100 frames, the assessment curve of the WY operator is relatively stable and robust to outliers. Overall, the q-ROFTrNYWA operator has better reliability and robustness in assessing online learning engagement, indicating that the q-ROFTrNDM method using the Yager operator is feasible.

5.5 *Comparative analysis of derived weight methods*

To further verify the effectiveness and feasibility of the CRITIC method, the CRITIC is replaced by Principal Component Analysis (PCA), the Expert Scoring Method (ESM), and the Factor Analysis (FA) method. Taking the feature data set of the first student as an example, the comparison of the results from each derived weight method is shown in Figure 6.

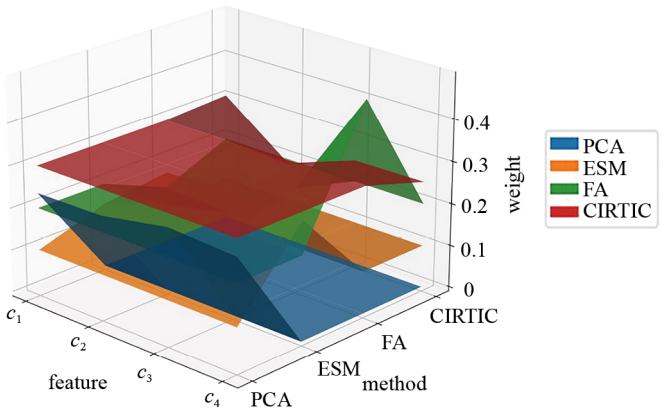

Figure 6. First student dataset-Comparison of feature scores for different methods

The comparison results in Figure 6 show that the CRITIC method is superior to the Principal Component Analysis (PCA), ESM, and FA methods for the first student. The results show that the weight distribution of the CRITIC method is highly consistent with that of the expert. The derived CRITIC method considers the relationship between four factors: body posture affects head posture, which in turn affects gaze and facial expression. This is consistent with actual online learning assessments and is therefore suitable for deriving the attribute weights for online learning. Especially in dynamic features such as head posture and body posture, the CRITIC method demonstrates its ability to overcome the limitations of traditional objective methods of ignoring feature correlations in this assessment.

Overall, the CRITIC method is more efficient than other traditional approaches in handling uncertainty and ambiguous environments due to its dynamic integration of feature information and correlation. Therefore, the CRITIC method is optimal compared to the method for assessing students' online learning engagement.

5.6 *Time complexity analysis*

To assess the time complexity of q-ROFTrNDM, we used the dataset from section 5.2, comprising data from students stu1 to stu5. The time consumed by the q-ROFTrNDM assessment method was recorded as q varied, and the average value of 10 repeated calculations for each student was taken as the result. The implementation was carried out on a personal computer (Intel Core i7-13700KF processor, clock frequency 3.40 GHz, 32 GB memory). The q-ROFTrNDM assessment method was implemented using Python 3.8, and the implementation results are shown in Figure 7.

As can be seen from Figure 7, the q-ROFTrNDM method exhibits stable performance, with minimal fluctuations across q values ranging from 2 to 9. The average assessment time for most students falls between 5 and 6 MS, all of which are less than 10 Ms. Consequently, the q-ROFTrNDM method boasts low time complexity, enabling rapid calculation of assessment results. Compared to existing artificial intelligence methods such as CNNs, the q-ROFTrNDM method has lower time complexity. However, the q-ROFTrNDM approach relies on expert assessment, which requires significant expert time for different students in various environments, resulting in poor generalization ability. Therefore, the q-ROFTrNDM method proposed in this paper is only suitable for small-sample expert assessment scenarios. Nevertheless, the accumulated expert assessment data can be effectively utilized for training artificial intelligence algorithms, yielding more reliable results.

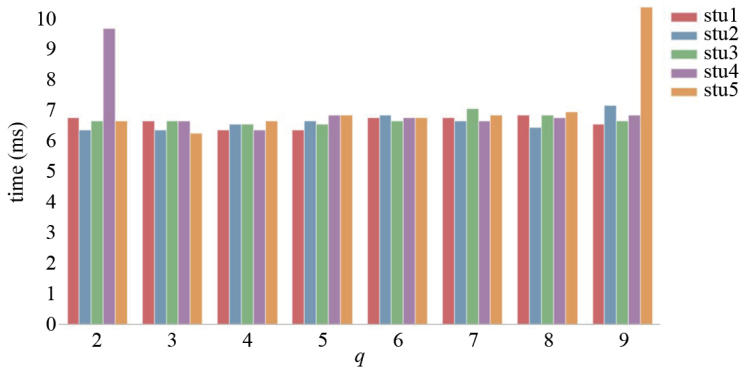

Figure 7. The time consumption of different students under different q values

6. Discussion

The q-ROFTrNDM method proposed in this study was developed within the q-ROFTrN environment; it can be effectively utilized for decision-making and assessment in ambiguous environments. Initially, the q-ROFTrNYWA operator was introduced, marking the first extension of the Yager operator to the q-ROFTrN context. This operator offers greater flexibility in handling uncertainty and fuzzy information, enhancing the expressiveness and adaptability of assessments. Furthermore, a derivative feature weighting method developed based on the CRITIC method in the q-ROFTrNs environment is proposed. This method not only overcomes the shortcomings of specifying weights but also possesses objectivity. The q-ROFTrNDM method integrates fuzzy distance, Yager operator, CRITIC method, and scoring function to achieve a comprehensive and dynamic assessment of student engagement. The sensitivity analysis results of the q-ROFTrNDM method show that the rankings of students remain consistent under different parameter settings (see Figures 3 and 4), indicating that the q-ROFTrNDM method has good stability. Compared with other operators, the q-ROFTrNYWA operator used in the q-ROFTrNDM method achieves the highest accuracy score (see Figure 5) and is

closest to the online engagement assessed by experts. Compared with other derived weight methods, the CRITIC method considers the relationship between four factors: body posture affects head posture, head posture affects gaze and facial expressions, which is consistent with actual online learning assessments and suitable for deriving the weight of online learning attributes (see Figure 6). At the same time, the computational time complexity of the q-ROFTrNDM method is less than 10 milliseconds (see Figure 7), making it efficient in small-scale fuzzy assessments. Therefore, based on the proposed q-ROFTrNYWA operator and CRITIC derived weight method, the q-ROFTrNDM method can be effectively used for assessing online learning engagement based on expert fuzzy assessment values.

Although the q-ROFTrNDM method excels in assessing online learning engagement under conditions of uncertainty, dynamism, and small-scale data, it relies on expert assessments of post-online learning videos. This approach hinders real-time, large-scale data assessment of student engagement, thereby limiting its application in real-time feedback scenarios. The primary reason is its dependence on expert assessments of collected data, which limits its strong generalization capabilities. Additionally, student engagement level labels in online learning rely on expert assessments. While these assessments carry a certain level of authority, they still suffer from subjective biases and fail to achieve automation and standardization in labeling. Compared to existing artificial intelligence methods such as CNNs, q-ROFTrNDM has lower computational complexity. However, it requires experts to assess student engagement, which can be time-consuming and costly for different students in various environments. Therefore, the q-ROFTrNDM method proposed in this paper is suitable for small-sample expert assessment scenarios. However, the accumulated expert assessment data can be effectively utilized for training artificial intelligence models, resulting in online learning assessment models with strong generalization capabilities and high accuracy for real-time engagement assessment.

To overcome the limitations of q-ROFTrNDM, the research team plans to combine the q-ROFTrNDM method with deep learning technology to construct and train an online learning engagement assessment model for real-time assessment of students' online learning engagement. Firstly, the research team will collect more online learning video data, segment, align, and annotate the video data, and then use the q-ROFTrNDM method to assess and verify the quality of the annotated data. Furthermore, by integrating the q-ROFTrNDM method with deep learning models (such as CNN, Transformer, etc.), a multi-modal engagement assessment model with high recognition accuracy, strong generalization ability, and lightweight will be developed to achieve efficient and real-time student engagement assessment.

7. Conclusion

An integrated q-ROFTrNDM method is developed in this paper to assess the online learning engagement based on q-ROFTrN. The q-ROFTrNYWA operator is designed, the Yager operator is firstly extended to the q-ROFTrN environment. The feature weights are derived based on the CRITIC method under the q-ROFTrNs environment, which not only overcomes the shortcomings of specified weights but also ensures objectivity. The developed q-ROFTrNDM method combines fuzzy distance, q-ROFTrNYWA operator, weights derivation method, and score function to achieve a comprehensive assessment of students' online learning engagement according to expert assessment values. The implementation results of the case show that q-ROFTrNDM can be effectively used to assess engagement in online learning. The q-ROFTrNDM assessment results show that students' online learning engagement is consistent with expert assessment results. Parameter sensitivity analysis results indicate that the proposed q-ROFTrNDM does not change the assessment results of the most engaged students. The comparative analysis results show that the q-ROFTrNDM has the highest engagement score, outperforming the comparison methods. The computing time of the q-ROFTrNDM method is lower by 10ms, resulting in a shorter assessment time. Therefore, the proposed q-ROFTrNDM is feasible and effective.

Although q-ROFTrNDM can effectively assess students' online learning engagement based on experts' assessment values, the q-ROFTrNDM method cannot adapt to large-scale student engagement assessment and is difficult to generalize directly. However, the assessment results of q-ROFTrNDM can provide high-quality data for machine learning and deep learning. Therefore, the team will integrate fuzzy assessment methods with neural network methods to train a more intelligent online learning engagement model as the focus of research.

Author contributions

Benting Wan: Supervision, Conceptualization, Data curation, Investigation, Methodology, Validation, Visualization, Writing-original draft. JiaChen Sun: Data curation, Methodology, Project administration, Resources, Writing-original draft, Writing-review &editing. Haifeng Du: Data curation, Investigation, Writing- review & editing. Jun Wan: Data curation and code writing, Formal analysis. Xiangwen Kong: Data collection, Software, Writing-review & editing. Youyu Cheng: Data curation, Formal • analysis, review • & • editing.

Funding

This paper is by the Ministry of Education Humanities and Social Sciences Planning Fund Project under Grant 22YJA880051, and in part by the Department of Education of Jiangxi Province of China under Grant GJJ2200535, 22YB052, JG2022055, and JXYJG-2022-94, and in part by Jiangxi Provincial Postgraduate Innovation Special Fund Projects under Grant YC2025-S473.

Data and code availability statement

The data and code that support the findings of this study are openly available in GitHub at https://github.com/JUN-WA/q_ROFTrNDM.

Ethics declaration

We have ensured that all participants provided written informed consent and have the right to withdraw from the study at any time. The collection and processing of research data comply with privacy protection principles, and all personally identifiable information has been removed or encrypted.

Conflict of interest

These authors declare that there have been no conflicts of interest among them.

References

[1] Larbani M, Aouni B. A generalized approach for multi-criteria decision aid methods. *Annals of Operations Research*. 2025; 346: 1187-1215. Available from: https://doi.org/10.1007/s10479-024-06327-4.

[2] Le M, Nhieu N. A behavior-simulated spherical fuzzy extension of the integrated multi-criteria decision-making approach. *Symmetry*. 2022; 14(6): 1136. Available from: https://doi.org/10.3390/sym14061136.

[3] Zadeh LA. Fuzzy sets. *Information and Control*. 1965; 8(3): 338-353. Available from: https://doi.org/10.1016/S0019-9958(65)90241-X.

[4] Atanassov KT. Intuitionistic fuzzy sets. *Fuzzy Sets and Systems*. 1986; 20(1): 87-96. Available from: https://doi.org/10.1016/S0165-0114(86)80034-3.

[5] Anh PV, Thuy NN, Cuong TH, Giang NL. Incremental attribute reduction with α, β-level intuitionistic fuzzy sets. *International Journal of Approximate Reasoning*. 2025; 176: 109326. Available from: https://doi.org/10.1016/j.ijar.2024.109326.

[6] Chen M, Lin W, Zhou L. Consistency analysis and priority weights for Pythagorean fuzzy preference relations. *IEEE Access*. 2020; 8: 89106-89116. Available from: https://doi.org/10.1109/access.2020.2990067.

[7] Ayyildiz E, Erdogan M, Gul M. A comprehensive risk assessment framework for occupational health and safety in pharmaceutical warehouses using Pythagorean fuzzy Bayesian networks. *Engineering Applications of Artificial Intelligence*. 2024; 135: 108763. Available from: https://doi.org/10.1016/j.engappai.2024.108763.

[8] Hussain R, Hussain Z, Sarhan NM, Juraev N, Ur Rahman S. Distance and similarity measures on belief and plausibility under *q*-rung orthopair fuzzy sets with applications. *Scientific Reports*. 2024; 14: 18959. Available from: https://doi.org/10.1038/s41598-024-66555-3.

[9] Banik AK, Dutta P, Pamucar D, Simic V. Enhanced information measures using *q*-Rung Orthopair Fuzzy Sets for improved criminal investigation techniques. *Engineering Applications of Artificial Intelligence*. 2026; 163: 112622. Available from: https://doi.org/10.1016/j.engappai.2025.112622.

[10] Zhu H, Zhao J, Li H. *q*-ROF-SIR methods and their applications to multiple attribute decision making. *International Journal of Machine Learning and Cybernetics*. 2022; 13: 595-607. Available from: https://doi.org/10.1007/s13042-020-01267-4.

[11] Du J, Zhu J. A decision support model for nursing chair design driven by patent literature analysis and trapezoidal fuzzy AHP. *International Journal of Industrial Ergonomics*. 2025; 110: 103811. Available from: https://doi.org/10.1016/j.ergon.2025.103811.

[12] Wan S. Power average operators of trapezoidal intuitionistic fuzzy numbers and application to multi-attribute group decision making. *Applied Mathematical Modelling*. 2013; 37(6): 4112-4126. Available from: https://doi.org/10.1016/j.apm.2012.09.017.

[13] Khatter K. Interval valued trapezoidal neutrosophic set: Multi-attribute decision making for prioritization of non-functional requirements. *Journal of Ambient Intelligence and Humanized Computing*. 2021; 12(1): 1039-1055. Available from: https://doi.org/10.1007/s12652-020-02130-8.

[14] Wan B, Huang J. A Choquet integral-based TODIM method for *q*-rung trapezoidal fuzzy numbers and its application in group decision-making. *International Journal of Intelligent Computing and Cybernetics*. 2023; 16(3): 545-573. Available from: https://doi.org/10.1108/IJICC-10-2022-0267.

[15] Bihari R, Jeevaraj S, Kumar A. Complete ranking for generalized trapezoidal fuzzy numbers and its application in supplier selection using the GTrF-CoCoSo approach. *Expert Systems with Applications*. 2024; 255: 124612. Available from: https://doi.org/10.1016/j.eswa.2024.124612.

[16] Lin J, Duan R, Tang W, Lian K, Chen H. Distributed optimization filtering for fuzzy quantization system with membership functions online learning. *Asian Journal of Control*. 2025; 27(5): 2606-2624. Available from: https://doi.org/10.1002/asjc.3613.

[17] Kang K, Xie J, Liu X, Wang H. Overview of the application of intelligent optimization algorithms in multi-attribute group decision making. *Applied Intelligence*. 2025; 55(409). Available from: https://doi.org/10.1007/s10489-025-06324-5.

[18] Razzaq A, Khan Z, Riaz M, Pamucar D. Sustainable decision support system in Industry 4.0 under uncertainties with m-polar picture fuzzy information aggregation. *Alexandria Engineering Journal*. 2024; 116: 271-295. Available from: https://doi.org/10.1016/j.aej.2024.11.104.

[19] Reddy G, Hait S, Guha D, Mahadevappa M. Classification of epileptic EEG signals with the utilization of Bonferroni mean based fuzzy pattern tree. *Expert Systems with Applications*. 2023; 239: 122424. Available from: https://doi.org/10.1016/j.eswa.2023.122424.

[20] Yalçın G, Kara K, Saygıner C, Simic V, Pamucar D. Selecting cloud providers of infrastructure as a service: A picture fuzzy symmetry point of criterion-based expert-driven model. *Engineering Applications of Artificial Intelligence*. 2025; 157: 111132. Available from: https://doi.org/10.1016/j.engappai.2025.111132.

[21] Shahzadi G, Akram M, Al-Kenani AN. Decision-making approach under Pythagorean Fuzzy Yager weighted operators. *Mathematics*. 2020; 8(1): 70. Available from: https://doi.org/10.3390/math8010070.

[22] Güner E, Aldemir B, Aydoğdu E, Aygün H. Novel Hamacher aggregation operators with applications to the AHP-COPRAS method for spherical fuzzy environment. *Neural Computing and Applications*. 2025; 37: 12941-12990. Available from: https://doi.org/10.1007/s00521-025-11167-9.

[23] Yao Z, Zhiping F. Method for multiple attribute decision making based on incomplete linguistic judgment matrix. *Journal of Systems Engineering and Electronics*. 2008; 19(2): 298-303. Available from: https://doi.org/10.1016/s1004-4132(08)60082-1.

[24] Wang Y, Wang W, Wang Z, Deveci M, Roy SK, Kadry S. Selection of sustainable food suppliers using the Pythagorean fuzzy CRITIC-MARCOS method. *Information Sciences*. 2024; 664: 120326. Available from: https://doi.org/10.1016/j.ins.2024.120326.

[25] Naz S, Ul Hassan MM, Mehmood A, Mehmood A, Espitia GP, Butt SA. Enhancing industrial robot selection through a hybrid novel approach: integrating CRITIC-VIKOR method with probabilistic uncertain linguistic *q*-rung orthopair fuzzy. *Artificial Intelligence Review*. 2024; 58(2): 59. Available from: https://doi.org/10.1007/s10462-024-11001-z.

[26] Gong K, Ma W, Lei W, Zhang H, Goh M. An individual satisfaction and influence measure-based approach for multi-attribute large-scale group decision-making with uncertain linguistic preference relations. *Computers & Industrial Engineering*. 2025; 201: 110888. Available from: https://doi.org/10.1016/j.cie.2025.110888.

[27] Rani P, Mishra AR, Deveci M, Antucheviciene J. New complex proportional assessment approach using Einstein aggregation operators and improved score function for interval-valued Fermatean fuzzy sets. *Computers & Industrial Engineering*. 2022; 169: 108165. Available from: https://doi.org/10.1016/j.cie.2022.108165.

[28] Getenet S, Cantle R, Redmond P, Albion P. Students' digital technology attitude, literacy and self-efficacy and their effect on online learning engagement. *International Journal of Educational Technology in Higher Education*. 2024; 21(3). Available from: https://doi.org/10.1186/s41239-023-00437-y.

[29] Liu Y, Ren J, Xu J, Bai X, Kaur R, Xia F. Multiple instance learning for cheating detection and localization in online examinations. *IEEE Transactions on Cognitive and Developmental Systems*. 2024; 16(4): 1315-1326. Available from: https://doi.org/10.1109/TCDS.2024.3349705.

[30] Guo X, Li W, Qiao J. A self-organizing modular neural network based on empirical mode decomposition with sliding window for time series prediction. *Applied Soft Computing*. 2023; 145: 110559. Available from: https://doi.org/10.1016/j.asoc.2023.110559.

[31] Zhi Y, Li J, Wang H, Chen J, Wei W. A multimodal sentiment analysis method based on fuzzy attention fusion. *IEEE Transactions on Fuzzy Systems*. 2024; 32(10): 5886-5898. Available from: https://doi.org/10.1109/TFUZZ.2024.3434614.

[32] Jiang Y, Dale R. Mapping the learning curves of deep learning networks. *PLOS Computational Biology*. 2025; 21(2): e1012286. Available from: https://doi.org/10.1371/journal.pcbi.1012286.

[33] Yager RR. Generalized orthopair fuzzy sets. *IEEE Transactions on Fuzzy Systems*. 2016; 25(5): 1222-1230. Available from: https://doi.org/10.1109/TFUZZ.2016.2604005.

[34] Wan B, Huang J, Zhang X. A modified TODIM based on compromise distance for MAGDM with *q*-rung orthopair trapezoidal fuzzy numbers. *Complexity*. 2021; 2021: 4269394. Available from: https://doi.org/10.1155/2021/4269394.

[35] Yager RR. Aggregation operators and fuzzy systems modeling. *Fuzzy Sets and Systems*. 1994; 67(2): 129-145. Available from: https://doi.org/10.1016/0165-0114(94)90082-5.

[36] Peng X, Liu L. Information measures for *q*-rung orthopair fuzzy sets. *International Journal of Intelligent Systems*. 2019; 34(8): 1795-1834. Available from: https://doi.org/10.1002/int.22115.

[37] Chen S, Tsai K. Multiattribute decision making based on new score function of interval-valued intuitionistic fuzzy values and normalized score matrices. *Information Sciences*. 2021; 575: 714-731. Available from: https://doi.org/10.1016/j.ins.2021.07.074.

[38] Chen T. A comparative analysis of score functions for multiple criteria decision making in intuitionistic fuzzy settings. *Information Sciences*. 2011; 181(17): 3652-3676. Available from: https://doi.org/10.1016/j.ins.2011.04.030.

[39] Jiang X, Chen X, Jiao Y, Zhang L. Objective evaluation of motion cueing algorithms for vehicle driving simulator based on criteria importance through intercriteria correlation (CRITIC) weight method combined with gray correlation analysis. *Machines*. 2024; 12(5): 344. Available from: https://doi.org/10.3390/machines12050344.

[40] Zaletelj J, Košir A. Predicting students' attention in the classroom from Kinect facial and body features. *EURASIP Journal on Image and Video Processing*. 2017; 2017(1): 80. Available from: https://doi.org/10.1186/s13640-017-0228-8.

[41] Jie W, Guanyu H, Xinyu Y, Luu AT, Dong Y. Learning facial expression and body gesture visual information for video emotion recognition. *Expert Systems with Applications*. 2023; 237: 121419. Available from: https://doi.org/10.1016/j.eswa.2023.121419.

[42] Mo J, Liang H, Yuan H, Shou Z, Zhang H. Learning attention characterization based on head pose sight estimation. *Multimedia Tools and Applications*. 2024; 83(38): 85917-85937. Available from: https://doi.org/10.1007/s11042-024-20204-z.

[43] Roshanzamir M, Jafari M, Alizadehsani R, Roshanzamir M, Shoeibi A, Gorriz JM, et al. What happens in face during a facial expression? Using data mining techniques to analyze facial expression motion vectors. *Information Systems Frontiers*. 2024. Available from: https://doi.org/10.1007/s10796-023-10466-7.

[44] Ali J, Rasool W. Interval-valued *q*-rung orthopair fuzzy Aczel-Alsina operations-based Bonferroni mean aggregation operators and their applications. *Computational and Applied Mathematics*. 2023; 43(1): 7. Available from: https://doi.org/10.1007/s40314-023-02511-7.

[45] Basu R, Chakraborty S, Saha AK. Novel *q*-rung orthopair fuzzy distance-based similarity measure and score function in real-life decision-making. *Engineering Applications of Artificial Intelligence*. 2025; 147: 110348. Available from: https://doi.org/10.1016/j.engappai.2025.110348.

[46] Zhang H, Wei G, Chen X. Spherical fuzzy Dombi power Heronian mean aggregation operators for multiple attribute group decision-making. *Computational and Applied Mathematics*. 2022; 41(3): 98. Available from: https://doi.org/10.1007/s40314-022-01785-7.

[47] Liu P, Wang P. Some interval-valued intuitionistic fuzzy Schweizer-Sklar power aggregation operators and their application to supplier selection. *International Journal of Systems Science*. 2018; 49(6): 1188-1211. Available from: https://doi.org/10.1080/00207721.2018.1442510.

[48] Tang X, Fu C, Xu DL, Yang S. Analysis of fuzzy Hamacher aggregation functions for uncertain multiple attribute decision making. *Information Sciences*. 2017; 387: 19-33. Available from: https://doi.org/10.1016/j.ins.2016.12.045.